



# Acoustic response and ambient pressure sensitivity characterization of SonoVue for noninvasive pressure estimation

Roozbeh H. Azami, <sup>1</sup> Flemming Forsberg, <sup>2</sup> John R. Eisenbrey, <sup>2</sup> and Kausik Sarkar<sup>1,a)</sup> Department of Mechanical and Aerospace Engineering, The George Washington University, Washington, DC 20052, USA

### **ABSTRACT:**

Subharmonic aided pressure estimation (SHAPE) is a noninvasive pressure measurement technique based on the pressure dependent subharmonic signal from contrast microbubbles. Here, SonoVue microbubble with a sulfur hexafluoride (SF<sub>6</sub>) core, was investigated for use in SHAPE. The study uses excitations of 25–700 kPa peak negative pressure (PNP) and 3 MHz frequency over eight pressurization cycles between atmospheric pressure and overpressures, ranging from 0 to 25 kPa (0 to 186 mm Hg). The SonoVue subharmonic response was characterized into two types. Unlike other microbubbles, SonoVue showed significant subharmonic signals at low excitations (PNPs, 25–400 kPa), denoted here as type I subharmonic. It linearly decreased with increasing overpressure (–0.52 dB/kPa at 100 kPa PNP). However, over multiple pressurization-depressurization cycles, type I subharmonic changed; its value at atmospheric pressure decreased over multiple cycles, and at later cycles, it recorded an increase in amplitude with overpressure (highest, +13 dB at 50 kPa PNP and 10 kPa overpressure). The subharmonic at higher excitations (PNP > 400 kPa), denoted here as type II subharmonic, showed a consistent decrease with the ambient pressure increase with strongest sensitivity of -0.4 dB/kPa at 500 kPa PNP. © 2024 Acoustical Society of America. https://doi.org/10.1121/10.0025690

(Received 29 November 2023; revised 21 March 2024; accepted 27 March 2024; published online 17 April 2024)

[Editor: Charles C. Church] Pages: 2636–2645

### I. INTRODUCTION

Contrast enhanced ultrasound (CEUS) has expanded ultrasound imaging applications to new diagnostic and therapeutic areas employing encapsulated gas microbubbles. <sup>1-4</sup> These microbubbles, with a diameter of 1–10  $\mu$ m and a gas core of sulfur hexafluoride (SF<sub>6</sub>) or various perfluorocarbon (PFC) gasses, are encapsulated in a shell made of proteins, lipids, or polymers. <sup>5</sup> Depending on the ultrasound excitation, they generate fundamental, harmonic, as well as sub- and ultra-harmonic signals. <sup>6-8</sup> Ambient pressure dependence of the subharmonic signal is being actively investigated for blood pressure monitoring. <sup>9-14</sup> Here, we investigate the pressure dependent subharmonic response from a SF<sub>6</sub> contrast microbubble, SonoVue/Lumason (Bracco Diagnostics, Princeton, NJ).

With minimal subharmonic signal from the tissue, subharmonic generated by contrast microbubbles can give rise to better contrast-to-tissue ratios in the subharmonic imaging (SHI) modality. <sup>15–20</sup> The typical subharmonic response from a microbubble is a threshold phenomenon, i.e., it is generated only above a certain excitation threshold (occurrence stage), then grows (growth stage) before saturating at higher excitations (saturation stage). <sup>9,15,21,22</sup> Based on the

observation that the subharmonic signal from microbubbles decreases linearly with the hydrostatic pressure, subharmonic aided pressure estimation (SHAPE), a noninvasive pressure measurement technique, was proposed and demonstrated in a canine model. SHAPE was successfully used in humans to diagnose portal hypertension with Sonazoid (GE Healthcare, Oslo, Norway) and measure intracardiac pressure with Definity (Lantheus Medical Imaging Inc., North Billerica, MA).

The contrast agent, SonoVue/Lumason, has been approved in North America, Europe, Asia, and Brazil for applications such as focal liver lesions characterization, left ventricular opacification and endocardial border delineation, and ultrasonography of urinary tract (applications vary in different countries). 5,24 Several studies have investigated its suitability for SHAPE, 25-32 leading, however, to widely varying results, including, sometimes, contradicting trends. For instance, Qiao et al.28 observed that subharmonic decreased with increasing pressure in the range 20-160 mm Hg (with the highest sensitivity of 1.84 dB/kPa at the growth stage of 346 kPa PNP, 5 MHz). However Nio et al.<sup>27</sup> reported a nonmonotonic, triphasic, increase in subharmonic at PNPs up to 300 kPa, 2-7 MHz, i.e., initial increase saturated and declined beyond 100 mm Hg overpressure. On the other hand, Xu et al.<sup>25</sup> reported two stages of growth with PNP at 4 MHz frequency, where the first stage is between 40 and 300 kPa,

<sup>&</sup>lt;sup>2</sup>Department of Radiology, Thomas Jefferson University, Philadelphia, Pennsylvania 19107, USA

a)Email: sarkar@gwu.edu

where subharmonic increased with overpressure (<40 mm Hg), followed by a saturation in 300–400 kPa and a second growth stage in 400–540 kPa PNP, where subharmonic decreased with overpressure. Note that increasing and decreasing trends were also reported in other PFC bubbles by Frinking *et al.*<sup>33</sup> and our group.<sup>34</sup> We found *in vitro* that at low excitations, overpressure lowers the threshold, leading to generation of subharmonic signal that is otherwise absent at atmospheric pressure, presumably due to buckling, <sup>35–38</sup> while at higher excitations, subharmonic already present at atmospheric pressure decreases with increasing overpressure, possibly due to oscillation restrictions or shrinkage of free gas bubbles. <sup>20,33,34</sup>

However, SonoVue presents a very different case than the laboratory-made PFC microbubble that we studied earlier.<sup>34</sup> The core gas SF<sub>6</sub> of SonoVue has a much lower molecular weight than PFCs and thereby has a substantially higher gas diffusivity. It results in significantly different dynamics as will be evident from the results, further justifying the present investigation. Unlike the PFC microbubbles, where the subharmonic change due to overpressure did not vary over multiple pressurization cycles and only their averages were, therefore, studied, here we notice different behaviors over multiple cycles, warranting detailed investigation of cycle dependence. Furthermore, previous pressure sensitivity studies of SonoVue were limited either in acoustic pressure or the overpressure range. In this study, we investigated the ambient pressure sensitivity in all stages of subharmonic production by using PNPs in 25-700 kPa range and 3 MHz frequency excitation under hydrostatic pressure cycles of 0-25 kPa, similar to physiological pressure range. Our findings also explicate previous contradictory observations. Due to the large number of parameters, the current investigation is restricted to a single frequency, which is representative of the resonance frequency of the polydisperse SonoVue agent as reported in the literature. 31,39,40 The pressure sensitivity of subharmonic response at different frequency was studied previously,<sup>34</sup> resulting in qualitatively similar behaviors.

### II. METHOD

SonoVue/Lumason microspheres contain a SF<sub>6</sub> gas core and an outer shell monolayer consisting of distearoylphosphatidyl-choline (DSPC) and dipalmitoylphosphatidylglycerol sodium (DPPG-Na) with palmitic acid as stabilizer. SonoVue microbubbles were activated following the vendor's instruction and immediately used in experiments within 2h of activation (they were found to be reasonably stable within a vial for this period, and it is in accordance with the product monograph). Activated microbubbles have concentrations of  $1.5-5.6 \times 10^8$  microbubble/mL and mean diameter range of 1.5-2.5 µm with 99% of bubbles smaller than  $10 \,\mu \text{m}$  (as indicated in the product monograph). For each experiment, a fresh 0.2 ml aliquot of activated SonoVue was drawn from the vial and diluted 1000 times into 200 ml of distilled water. Then, 120 ml of the diluted suspension, containing about  $1.5-5.6 \times 10^{5}$  microbubbles/mL, was transferred into the pressurizing chamber made of a 3D-printed box  $(40 \text{ mm wide} \times 40 \text{ mm high} \times 45.2 \text{ mm} \text{ deep})$  with acoustically transparent windows for transmitting and receiving ultrasound [Fig. 1(a)]. The box was filled up to a level that submerged the windows, and a small air gap would remain between the liquid and ceiling, and the ambient pressure adjustment inside the chamber was performed using an air-filled syringe. Details of the pressurizing chamber and experimental setup are described in our previous paper.<sup>34</sup>

To study the effects of ambient pressure on the acoustic behavior of SonoVue, the pressurizing box, consisting of the microbubble suspension, was placed in the measurement tank filled with distilled water. Two ultrasonic focused

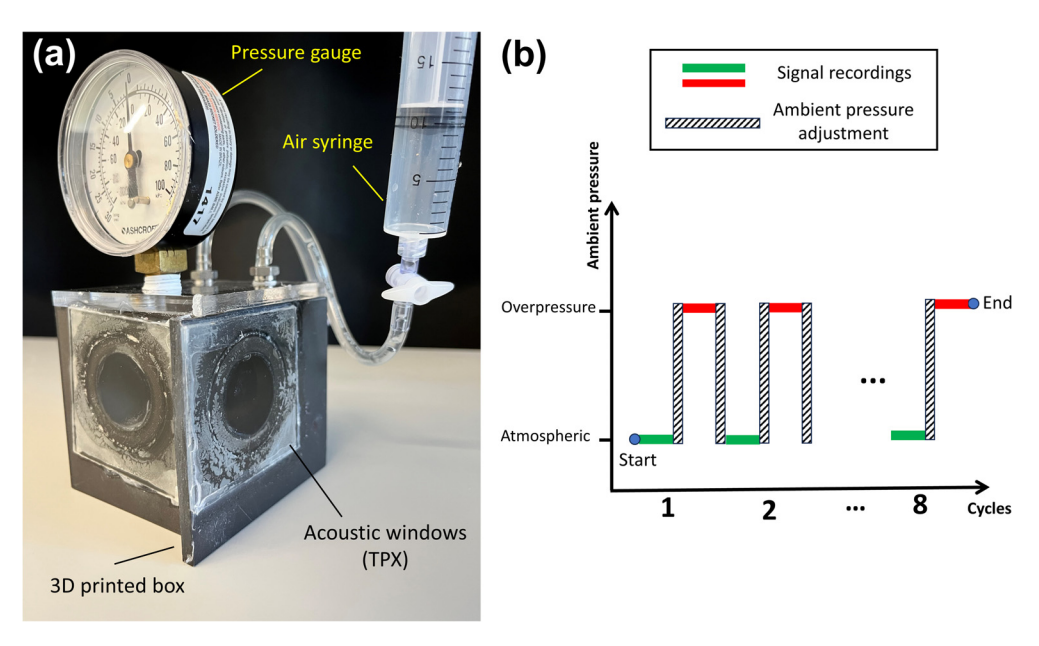


FIG. 1. (Color online) (a) Pressurizing chamber and (b) recording sequence in the experiment are shown. At each cycle, bubbles response was recorded once at atmospheric pressure and once at overpressure.

transducers were fixed perpendicularly on the tank wall with their focal zone overlapping inside the pressurizing box. A magnetic bar placed inside the pressurizing chamber was driven at low speed by a magnetic stirrer (Fisher Scientific, Hampton, NH) to keep the suspension homogenous and replenish bubbles in the focal zone to minimize any effect of destruction caused by an ultrasound pulse. Microbubbles were interrogated by acoustic excitations of 3 MHz frequency and 25-700 kPa PNP produced by the 5 MHz single element focused transducer (V309, Olympus, Waltham, MA), driven by sine bursts of 32 cycles and 100 Hz pulse repetition frequency from arbitrary wave generator (DG1022, RIGOL, Portland, OR). Sine bursts were amplified by a 55 dB power amplifier (A150, Electronics and Innovation, Rochester, NY) before reaching the transmit transducer. The scattered response of SonoVue microbubble was received by the broadband focused transducer (Y-102, Sonic Concepts, Bothell, WA) connected to an ultrasonic pulser-receiver (Model 5800, Panametrics, Olympus, Waltham, MA) in receiving mode with a 20 dB gain. The conditioned signal was digitized and displayed in real time by an oscilloscope (MDO 3024, Tektronix, Beaverton, OR) in sample mode. At each recording, 20 voltage time signals were saved using a MATLAB (The MathWorks, Natick, MA) script. Signals were then multiplied by a hamming window of 10000 points, based on the oscilloscope record length. The frequency domain of the signal was calculated using fast Fourier transform with 16384 points. To calculate the dB values, the first half of the amplitude array was used, and 1 V amplitude was taken as the reference signal amplitude. The dB values of 20 signals were averaged to report as a single value for 1 recording.

Each experiment trial included a fresh diluted mixture of SonoVue microbubbles undergoing eight sequences of pressurizing and depressurizing cycles to a fixed overpressure magnitude [Fig. 1(b)]. At each cycle, response of microbubbles to a specific PNP (fixed during eight cycles) was recorded starting at atmospheric pressure [no overpressure applied; green sections in Fig. 1(b)]. Then, ambient overpressure was increased to a fixed value (5, 10, 15, 20, or 25 kPa equivalent to 37.5, 75, 112.5, 150, and 187.5 mm Hg) for recording at the static overpressure [red sections in Fig. 1(b)], which was released abruptly before the next cycle. A control measurement (0 kPa overpressure) corresponds to repeated measurements with no pressurization following the same recording sequence as above. A total of 16 recordings (8 at atmospheric pressure and 8 at the overpressure) were taken over 3 min (total operation time of one cycle was about 22.5 s; each recording lasted 5 s and the rest of the time was spent on adjusting the overpressure setting). Note that a similar procedure followed in our previous study of PFC bubbles<sup>34</sup> to obtain eight repeated readings of the experiments corresponding to one overpressure level resulted in similar subharmonic change due to overpressure in each repeat and, therefore, were averaged over eight cycles. However, here, for SonoVue with a SF6 core, we found significantly different responses over eight cycles,

leading us to study cycle dependence. Afterward, the microbubbles suspension was discarded. Experiment trials at each setting (overpressure and PNP) were replicated three times.

Data analysis was conducted using PYTHON programming language (version 3.9) along with the open-source libraries Pandas, SciPy, and NumPy. Throughout the analysis, average values were calculated based on three samples (n=3), and error bars were used to represent one standard deviation from the average. To calculate the change in subharmonic with overpressure, the subharmonic amplitude recorded at atmospheric pressure was subtracted from that recorded at overpressure part of the same cycle. Student t-test was used to evaluate the statistical significance (p-value < 0.05) between response at overpressure and atmospheric pressure. Additionally, it was used to evaluate the significance of the response at different cycles compared to the first cycle. Analysis of variance (ANOVA) was used to probe statistical significance between response of different groups at each cycle. Linear regression analysis was applied to establish the correlation between ambient pressure and acoustic response, and coefficient of determination  $(R^2)$  value was used to evaluate the goodness of predictability of ambient pressure by the change in subharmonic.

#### III. RESULTS

Figure 2 shows the response of freshly diluted SonoVue microbubbles to 3 MHz acoustic excitation at atmospheric pressure in the first pressurizing cycle (no previous overpressure). As depicted in Fig. 2(a), the subharmonic curve as a function of PNP shows considerable subharmonic generation even at excitations as low as 25 kPa. As a result, the subharmonic profile of SonoVue does not exhibit the three stage S-curve plot that was often observed with other bubbles as reported in the literature for lipid coated microbubbles. 8,15,21,22,34 Figure 2(b) illustrates the scattered power spectrum from SonoVue at 25 kPa excitation. Although there are weak higher harmonic responses, the subharmonic peak is noticeable above the noise floor at 1.5 MHz frequency. At higher excitations, one sees harmonic and ultraharmonic peaks as is commonly observed for other types of lipid microbubbles<sup>8,41,42</sup> [Fig. 2(c)].

In this study of SonoVue, we do not observe the three stages of subharmonic microbubble signals, occurrence, growth, and saturation, characteristic of many microbubbles. Instead, we notice subharmonic production even at relatively low excitation amplitudes of 25 kPa. Subharmonic at these low amplitudes (25–400 kPa), here noted as type I subharmonic, behaves differently under pressurization cycles from those at excitation amplitudes higher than 400 kPa, here called type II subharmonic (compare Fig. 3 and Fig. 5 for type I and type II examples; 200 kPa PNP vs 700 kPa PNP, respectively). The range of type II behavior coincides with typical growth and saturation stages of subharmonic generation of other microbubbles. Similar subharmonic profiles and stages of production are reported for SonoVue by Xu *et al.*<sup>25</sup>

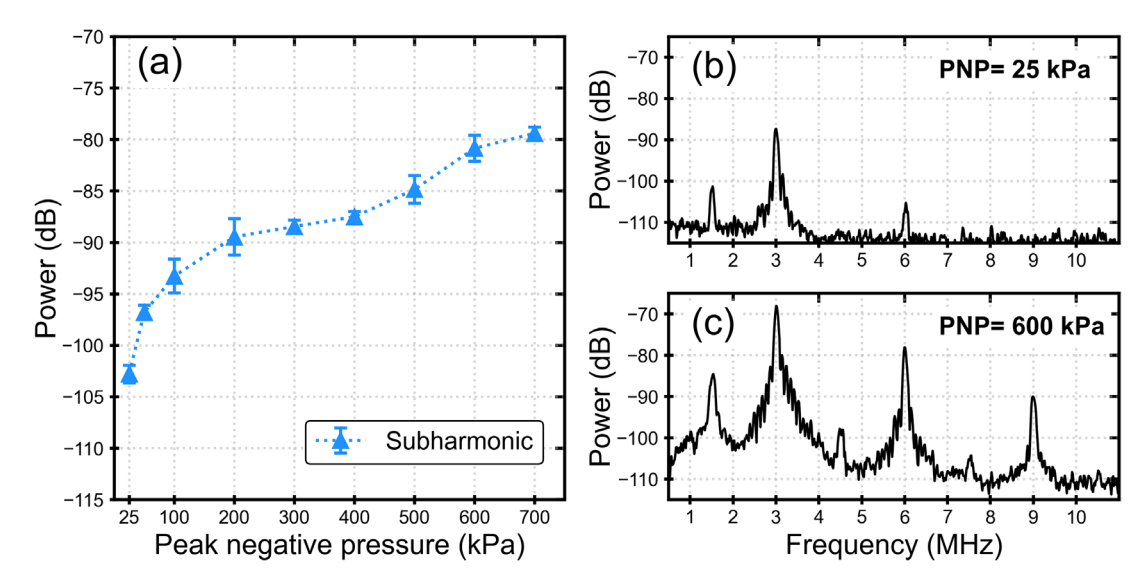


FIG. 2. (Color online) (a) Subharmonic response of SonoVue microbubbles as a function of the peak negative pressure (PNP) is shown. SonoVue exhibits two stages of subharmonic production before (type I) and after (type II) 400 kPa PNP. Example power spectrum of the scattered response, demonstrating subharmonic peak at 1.5 MHz is plotted at (b) 25 kPa and (c) 600 kPa PNP.

In Fig. 3, we show the baseline (recorded at atmospheric pressure) subharmonic response to 200 kPa PNP (type I) when the bubble is subjected to eight pressurizing-depressurizing cycles of different overpressures. For higher overpressure levels, the subharmonic gradually decays over successive pressurizing-depressurizing cycles, fastest at 25 kPa, eventually reaching the noise level after only two

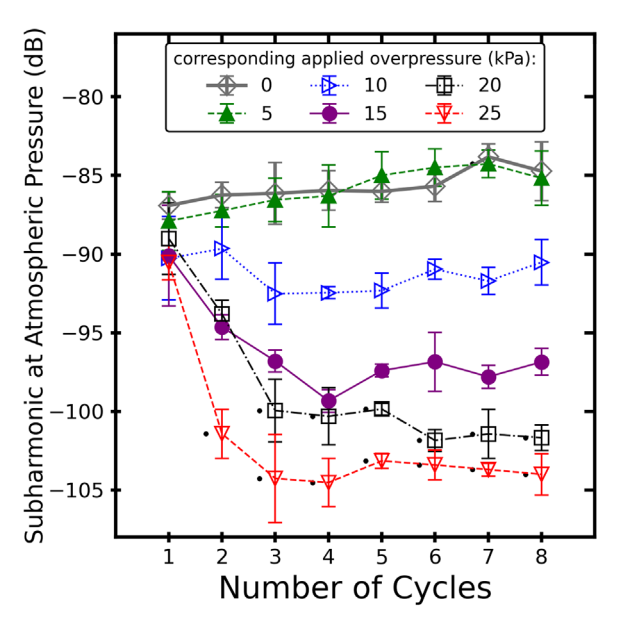


FIG. 3. (Color online) Example type I subharmonic response (PNP =  $200\,\mathrm{kPa}$ ) recorded at atmospheric pressure [green sections of Fig. 1(b)], corresponding to pressurizing depressurizing cycles of different overpressure magnitude [0 (i.e., control measurement with no overpressure application), 5, 10, 15, 20, and 25 kPa equivalent to 0, 37.5, 75, 112.5, 150, and 187.5 mm Hg]. Depending on the overpressure magnitude, initial baseline subharmonic amplitude diminishes after a few cycles of pressurization. Statistical significance (p-value < 0.05) of the difference from the first cycle is noted by a small dot near the corresponding datapoint.

cycles, while exhibiting no decay in the absence of overpressure (0kPa) or at 5kPa during the entire time (eight cycles). The statistical *t*-test reveals that for 20 and 25kPa pressurizing cycles, subharmonic at later cycles is significantly different compared to the first cycle. Additionally, ANOVA test did not find any significant difference between the values recorded at the first cycle for different groups, which emphasizes that different batches and fresh suspensions of bubbles exhibited similar responses before application of different overpressures. In other words, type I subharmonic of SonoVue is significantly affected by pressurizing-depressurizing cycles of high overpressures and disappears after a sufficient number of cycles.

Figure 4(a) further shows the effects of overpressure on subharmonic at atmospheric pressure, recorded with 0 kPa overpressure [green sections of Fig. 1(b)] and at 20 kPa overpressure [recorded in red section of Fig. 1(b)] during eight cycles of pressurizing-depressurizing at 200 kPa PNP. In the first cycle, applying overpressure decreases the subharmonic amplitude, but in later cycles, as baseline subharmonic (at 0 kPa overpressure) decreases, applying overpressure increases subharmonic, switching the trend. Figures 4(b) and 4(c) further demonstrate this change of trend in the effect of overpressure on subharmonic. Figure 4(b) illustrates the subharmonic peak at the atmospheric pressure decreases with overpressure. However, Fig. 4(c) shows that after multiple overpressure cycles, e.g., in the sixth cycle, the subharmonic peak at the atmospheric pressure has decayed to the noise level, and applying overpressure then results in subharmonic enhancement.

Figure 5 depicts a case of type II subharmonic, i.e., at a higher acoustic excitation, at 700 kPa. Unlike type I subharmonic (Fig. 3), at atmospheric pressure, it does not decay with cycles for any overpressure levels, instead, it increases over cycles. The student *t*-test confirmed the significance of difference in subharmonic in later cycles compared to the

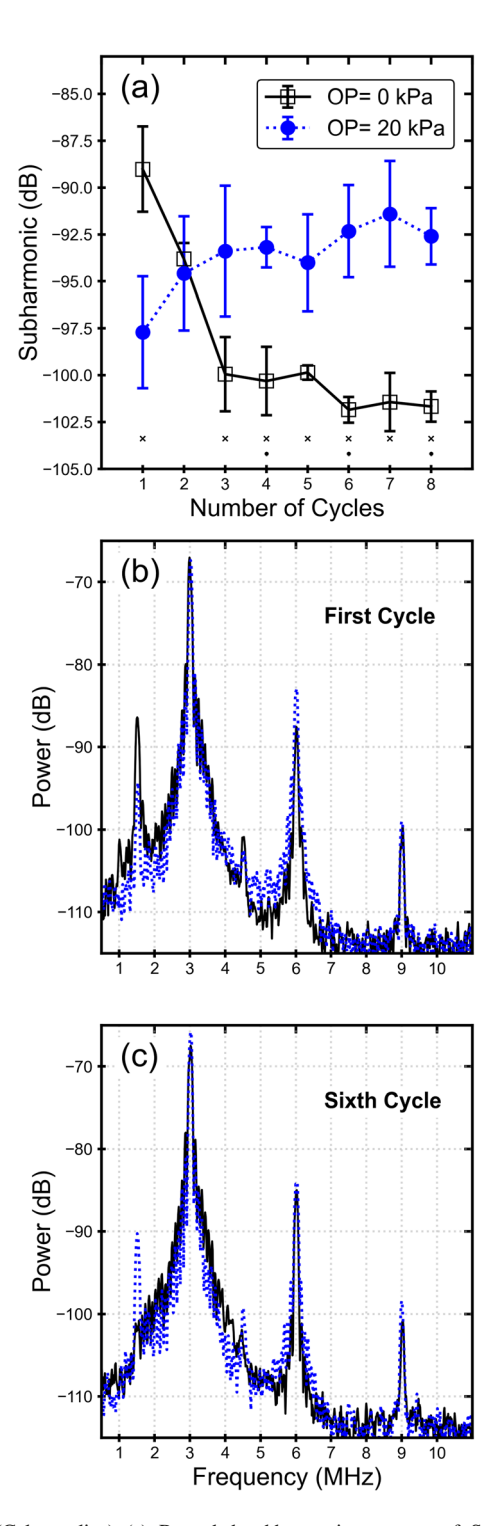


FIG. 4. (Color online) (a) Recorded subharmonic response of SonoVue at 200 kPa PNP acoustic excitation over eight pressurizing cycles is shown. The statistical significance (*p*-value < 0.05) of difference between baseline subharmonic [green section of Fig. 1(b)] and subharmonic at overpressure [red sections of Fig. 1(b)] is noted above the corresponding cycle by a small dot when linear values were compared and a small cross when dB values were compared. Frequency responses of SonoVue in (b) first and (c) sixth cycles are shown at 20 kPa overpressure (blue dotted line) and atmospheric pressure (black solid line).

first cycle (corresponding data point marked by a small dot). However, this difference has not shown any dependency on the relative overpressure magnitude as ANOVA test found no significant difference between groups at each cycle.

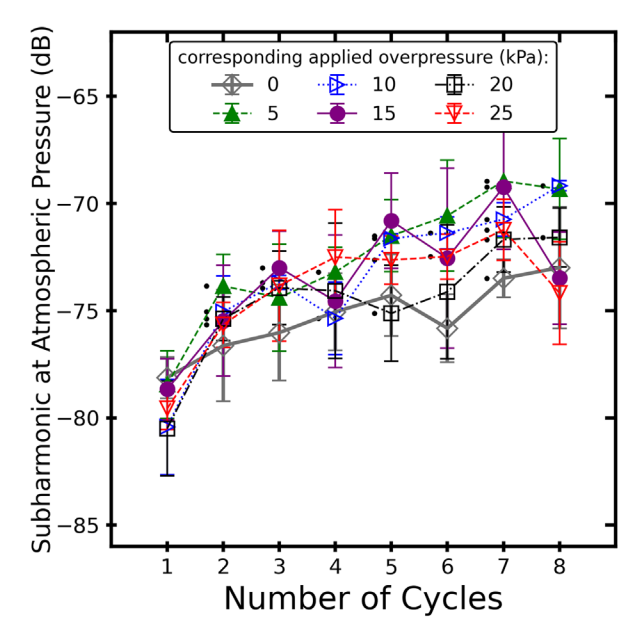


FIG. 5. (Color online) Effects of pressurizing cycles on type II baseline [recorded at atmospheric pressure, i.e., green sections in Fig. 1(b)] subharmonic at 700 kPa PNP. ANOVA test at each cycle confirms no dependency on different overpressure magnitude [0 (i.e., control measurement), 5, 10, 15, 20, and 25 kPa equivalent to 0, 37.5, 75, 112.5, 150, and 187.5 mm Hg]. Statistical significance (p-value < 0.05) of the difference from the first cycle is noted by a small dot near the corresponding datapoint.

Figure 6 displays the subharmonic response at acoustic excitation of 700 kPa at atmospheric pressure as well as at overpressure of 20 kPa over eight cycles. Unlike type I subharmonic shown in Fig. 4, applying overpressure leads to a consistent decrease in subharmonic for all eight cycles. The statistical significance (*p*-value < 0.05) of this decrease is marked above the corresponding cycles. Figures 6(b) and 6(c) compare the response at the first and sixth pressurizing cycles, respectively. In both, the subharmonic decreases with overpressure, and no change of trend is perceived as was observed for type I subharmonic [compare the change in subharmonic peak amplitude in Figs. 4(c) and 4(b)].

Because type I subharmonic decays and stabilizes after about four pressurizing cycles (Fig. 3) for all hydrostatic pressures, we report the ambient pressure sensitivity of the SonoVue subharmonic response (type I and type II) as an average of the measurements over the fifth through eighth cycles and compare them to the initial trend in the first cycle in Fig. 7 to emphasize how the ambient pressure sensitivity changes trend during pressurizing cycles for type I subharmonic. In Fig. 7(a), the subharmonic change with overpressure, averaged over the last four cycles, shows a nonmonotonic trend, which first increases followed by a decrease for type I (PNP  $\leq 400 \, \text{kPa}$ ) and a linear decreasing trend for type II (PNP > 400 kPa). This behavior is similar to our observation with an experimental lipid coated microbubble with C<sub>4</sub>F<sub>10</sub> gas core. 34 In other words, after four pressurization-depressurization cycles, the SonoVue behavior is identical to  $C_4F_{10}$  microbubbles. The sensitivity trend in the first cycle, shown in Fig. 7(b), however, is generally decreasing for low PNPs, which is special to SonoVue.

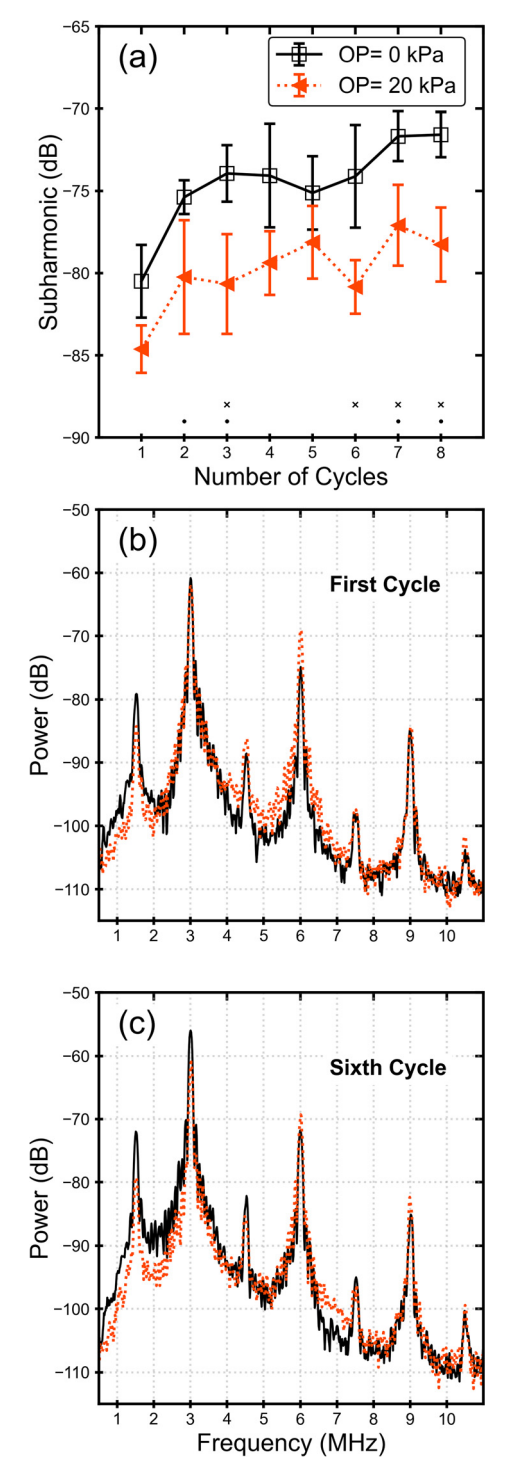


FIG. 6. (Color online) (a) Recorded subharmonic response of SonoVue at  $700\,\mathrm{kPa}$  acoustic excitation over eight cycles of  $20\,\mathrm{kPa}$  pressurizing is shown. The statistical significance (p-value < 0.05) of difference between baseline subharmonic [green section of Fig. 1(b)] and subharmonic at overpressure [red sections of Fig. 1(b)] is noted above the corresponding cycles by a small dot when linear values were compared and a small cross when dB values were compared. Frequency responses in (b) first and (c) sixth pressurizing cycles are shown at  $20\,\mathrm{kPa}$  overpressure (orange dotted line) and atmospheric pressure (black solid line).

This further underscores the difference in pressure sensitivity between type I subharmonic (25–400 kPa PNPs), which changes over cycles, and type II subharmonic (500–700 kPa PNPs), which remains the same.

### IV. DISCUSSION

SonoVue microbubbles are a potential candidate for use in the SHAPE as it is an approved agent for CEUS. However, variations in the subharmonic and its ambient pressure sensitivity, which was observed in previous studies, demanded an in-depth characterization of SonoVue acoustic behavior. In this study, we identified the following conditions for subharmonic production and ambient pressure sensitivity trends.

### A. Subharmonic generation at low PNPs (type I)

Unlike other lipid coated microbubbles that exhibited subharmonic signals only beyond a threshold of around 200–500 kPa, 15,22,43,44 Sono Vue has shown considerable subharmonic response at acoustic excitation amplitudes as low as 25 kPa (Fig. 2). Previous investigations have revealed that microbubbles with SF<sub>6</sub> gas core are more prone to generate subharmonic than those with  $C_3F_8$  and  $C_4F_{10}$  cores.<sup>45</sup> Higher diffusivity of SF<sub>6</sub> causes immediate shrinkage of microbubble on suspension caused by outward diffusion of the gas core, leading to a buckled lipid shell. 46,47 A buckled lipid shell has been revealed to be more susceptible to subharmonic generation in comparison to an elastic shell before buckling, 36,37 likely due to the fact that the rapid change in shell elasticity near buckling promotes compression-only behavior and subharmonic production. 35,38,48 The diffusion of SF<sub>6</sub> gas and resulting buckling may be responsible for the subharmonic generation at low PNPs for SonoVue.

### B. Type I subharmonic disappears under high hydrostatic pressure cycles

As was observed in Fig. 3, the type I subharmonic generated at low excitation amplitudes disappears after a few cycles of high hydrostatic pressurization (>10 kPa). The higher the maximum overpressure, the smaller number of pressurizingdepressurizing cycles was needed for subharmonic to decay to noise level. Note that the unchanged subharmonic level in the control experiment (0 kPa overpressure) over the eight cycles indicates no natural or excitation-induced dissolution of bubbles. 46,47 In addition, with baseline (atmospheric) fundamental and harmonic responses remaining also at a constant level [Figs. 4(b) and 4(c)], decay in subharmonic alone cannot be entirely due to destruction of bubbles under high hydrostatic pressure. Nio et al.<sup>27</sup> reported experimental observations at PNPs in the range 70-320 kPa and 5 MHz excitation, which shows that prior exposure of SonoVue to 150-200 mm Hg (20–25 kPa) of overpressure for 1 min resulted in a decrease in subharmonic at atmospheric pressure. This is in conformity with what we see in type I, i.e., subharmonic at atmospheric pressure decreases over several pressurization cycles. With hydrostatic pressure variation, they started the recording sequence from a high value of 25 kPa overpressure down to 0 kPa and observed first increasing subharmonic until 15 kPa overpressure and then a decrease until atmospheric pressure. It matches with our observation in Fig. 7(a) for the later cycles and our previous study.34

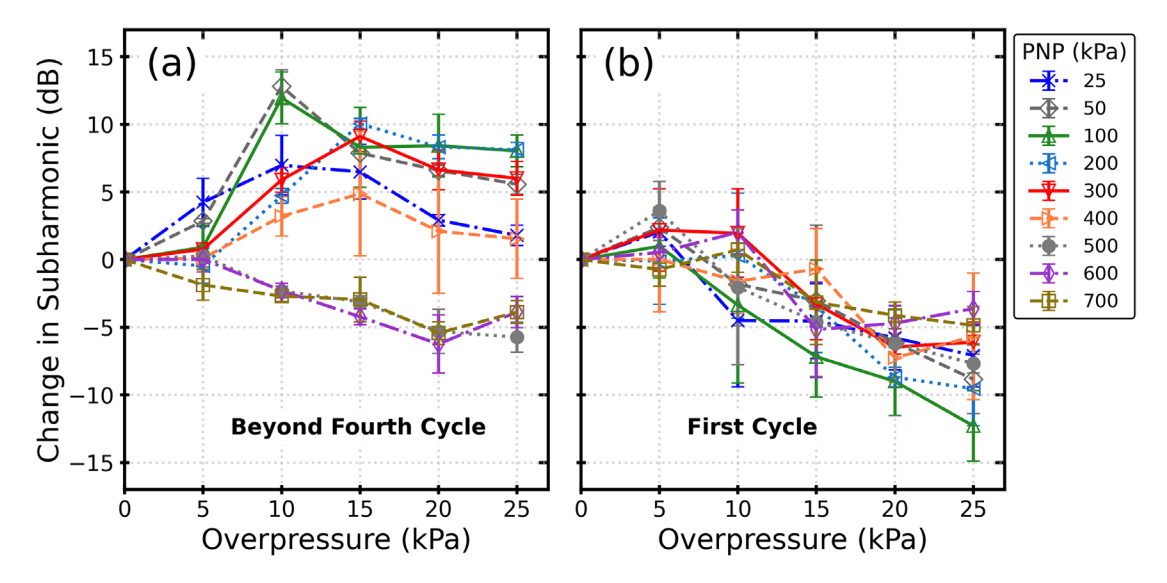


FIG. 7. (Color online) Subharmonic sensitivity of SonoVue depicted as the change in subharmonic amplitude after applying overpressure as a function of overpressure for different acoustic PNPs. (a) Averaged over measurements beyond the fourth pressurizing cycle (the fifth through eighth) and (b) measured at first cycle. The correlation between subharmonic and overpressure changes from negative at first cycle to positive in later cycles for type I subharmonic (PNP < 400 kPa).

As we noted above, subharmonic generation has been related to buckled shell of a contrast microbubble.<sup>36,37</sup> We feel that the observed behaviors, here, of SonoVue can be thought to be caused by elastic shell buckling and buckled shell transition back to an elastic regime caused by overpressure. The higher diffusivity of SF<sub>6</sub> in SonoVue facilitates this transition. As an easy buckling of shell gives rise to lower subharmonic threshold, here, a return of the microbubble from a buckled state to an elastic state, which is less prone to generate subharmonic at low excitation amplitude, causes an apparent decay of subharmonic. Two possible mechanisms for such a transition can be suggested. First, squeezing an already buckled microbubble under high overpressure results in shedding of excess lipid, which, in turn, removes the wrinkles (buckling) and forms an elastic shell, where the process is more intense under higher hydrostatic compressions, which explains the dependency of subharmonic decay rate to the maximum overpressure. Second, buckled SonoVue microbubbles inflate and transition into an elastic regime because of the diffusion of surrounding dissolved gas into a microbubble at high ambient pressure during the release of overpressure in a pressurizingdepressurizing cycle. Here, also the process can be facilitated under stronger pressurizing-depressurizing cycles. Both explanations conform with the reduction in type I subharmonic (Fig. 3) with cycles and its dependence on the overpressure amplitude.

### C. Two different correlations with ambient pressure in type I

Initially, type I subharmonic decreases with ambient pressure increase [Fig. 7(b)]. The highest sensitivity was  $-0.52 \, \text{dB/kPa}$  for  $100 \, \text{kPa}$  PNP at the first cycle with the determination coefficient ( $R^2$ ) of 0.94, which hints at a strong correlation. This value is comparable to previous

values for a decreasing trend (Table I in Azami et al.<sup>34</sup>) observed in the literature. However, as noted before, the subharmonic at atmospheric pressure disappeared after about four cycles of pressurizing (Fig. 3). Applying overpressure then (from the fifth cycle on), we see a subharmonic increase [Fig. 7(a)]. This observation agrees well with our previous study that showed overpressure enhances subharmonic if it is close to noise level at atmospheric pressure and decreases subharmonic if it already exists at atmospheric pressure.<sup>34</sup> In addition, similar to previous studies, 27,34 we see ascending and descending trends with maximum enhancement in subharmonic happening at overpressure in the range of 10-15 kPa. Here, we report the strongest enhancement of ~13 dB happening at 50 kPa PNP and 10 kPa overpressure measured after the fourth cycle of pressurizing.

### D. Type II subharmonic (at high PNPs) shows consistent ambient pressure sensitivity

The strong type II subharmonic at high acoustic excitations (above PNP 400 kPa) from SonoVue decreases with overpressure consistently for all cycles, unlike for cases with lower excitations. This observation agrees with our previous study and the typical behavior often observed with other microbubbles. Typical clinical applications use such high PNPs to detect adequate signal *in vivo*. The strongest sensitivity of type II subharmonic is  $-0.4\,\mathrm{dB/kPa}$  for  $500\,\mathrm{kPa}$  PNP ( $R^2 = 0.80$ ) in the first cycle [Fig. 7(b)] and  $-0.26\,\mathrm{dB/kPa}$  for  $500\,\mathrm{kPa}$  PNP ( $R^2 = 0.94$ ) in pressurizing cycles beyond the fourth cycle [Fig. 7(a)]. These values are in strong agreement with Andersen and Jensen<sup>32</sup> and Sun *et al.*<sup>49</sup>

Using the SHAPE method, an optimal acoustic output is selected by identifying the maximum gradient of the sub-harmonic amplitude as a function of acoustic pressure. 50,51

It was observed that subharmonic amplitude shows the strongest sensitivity to overpressure at this inflection point.<sup>9,51</sup> In this study, we show that SonoVue exhibits two local maxima gradients in different regions [Fig. 2(a)]: one at low PNP around 25-50 kPa and one at high PNP around 400-600 kPa. Therefore, the selected optimal acoustic output during this behavior may rely on the scanner sensitivity, where the lower inflection point occurs closer to the noise floor. This may result in totally different SHAPE sensitivities as our results show type I subharmonic happening at 25-400 kPa behaves differently compared to type II subharmonic. These findings, overall, match well with the literature, where studies using low PNP local maximum gradient observed an increase in subharmonic with overpressure<sup>27</sup> and those using high PNP local maximum reported a decrease in subharmonic with overpressure.<sup>28,32</sup>

Type II subharmonic offers a consistent correlation with ambient pressure over the cycles, however, with a lower sensitivity compared to type I and other clinical agents currently used in SHAPE, such as Sonazoid, <sup>13</sup> which might be a drawback in certain applications where high sensitivity is needed. In addition, type I subharmonic generation under overpressure suggests a medical go/no-go gauge concept for screening test of portal hypertension similar to Machado *et al.*<sup>52</sup> However, the complex variations (Fig. 7) with cycles (i.e., time) in type I subharmonic poses a drawback for pressure estimation, particularly in cardiac pressure estimation, where microbubbles would be expected to experience a number of cycles of overpressure with large variations (i.e., 10-25 kPa or 75-175 mm Hg). Note that the multiple pressurization and depressurization cycles are not intended to mimic the cardiac cycle. Yet, the cycle dependence observed here signals its importance in contrast imaging with SonoVue and its application in SHAPE. It should be remarked that the present study being in a static setup does not account for the effect of circulation in the cardiovascular system. However, our previous studies<sup>53–55</sup> reported similar SHAPE results at static pressure chamber and dynamic flow loop setup. Whereas the absolute values of the subharmonic amplitude, its threshold, and sensitivity to ambient pressure might change slightly for varying flow conditions, we believe that the mechanical and physical features exhibited here will be observed in a dynamic flow condition as well.

In conclusion, SonoVue, as a clinically approved ultrasound contrast agent, is a potential candidate for use in SHAPE. In this study, we showed that the subharmonic generation of SonoVue as a function of excitation pressure displayed two types of behavior depending on the excitation amplitude. Type I subharmonic generated at low PNPs (25–400 kPa) was exhibited to decrease with overpressure initially, but as its atmospheric pressure value declines to noise level over multiple pressurization-depressurization cycles (overpressure > 10 kPa), it increases with overpressure in the later cycles. In contrast, type II subharmonic generated at high PNPs (>400 kPa) shows a consistent decreasing behavior over many cycles with overpressure.

These findings may be key in determining and using the subharmonic signal amplitude for noninvasive pressure measurements.

### **ACKNOWLEDGMENTS**

K.S., F.F., and J.R.E. acknowledge partial support from National Institutes of Health Award No. R01EB032333. K.S. acknowledges partial support from National Science Foundation Award No. 1239105.

### AUTHOR DECLARATIONS Conflict of Interest

The authors have no conflict of interest to disclose.

### **DATA AVAILABILITY**

The data that support the findings of this study are available from the corresponding author upon reasonable request.

- <sup>1</sup>C. D. Malone, D. T. Fetzer, W. L. Monsky, M. Itani, V. M. Mellnick, P. A. Velez, W. D. Middleton, M. A. Averkiou, and R. S. Ramaswamy, "Contrast-enhanced US for the interventional radiologist: Current and emerging applications," Radiographics 40, 562–588 (2020).
- <sup>2</sup>J. R. Eisenbrey and F. Forsberg, "Contrast-enhanced ultrasound for molecular imaging of angiogenesis," Eur. J. Nucl. Med. Mol. Imag. **37**(Suppl 1), 138–146 (2010).
- <sup>3</sup>A. Salib, E. Halpern, J. Eisenbrey, T. Chandrasekar, P. H. Chung, F. Forsberg, and E. J. Trabulsi, "The evolving role of contrast-enhanced ultrasound in urology: A review," World J. Urol. **41**, 673–678 (2023).
- <sup>4</sup>J.-B. Liu, G. Wansaicheong, D. A. Merton, F. Forsberg, and B. B. Goldberg, "Contrast-enhanced ultrasound imaging: State of the art," J. Medical Ultrasound 13, 109–126 (2005).
- <sup>5</sup>P. Frinking, T. Segers, Y. Luan, and F. Tranquart, "Three decades of ultrasound contrast agents: A review of the past, present and future improvements," Ultrasound Med. Biol. 46, 892–908 (2020).
- <sup>6</sup>N. de Jong, A. Bouakaz, and P. Frinking, "Basic acoustic properties of microbubbles," Echocardiography **19**, 229–240 (2002).
- <sup>7</sup>B. Helfield, "A review of phospholipid encapsulated ultrasound contrast agent microbubble physics," Ultrasound Med. Biol. **45**, 282–300 (2019).
- <sup>8</sup>W. T. Shi and F. Forsberg, "Ultrasonic characterization of the nonlinear properties of contrast microbubbles," Ultrasound Med. Biol. 26, 93–104 (2000).
- <sup>9</sup>W. Shi, F. Forsberg, J. Raichlen, L. Needleman, and B. B. Goldberg, "Pressure dependence of subharmonic signals from contrast microbubbles," Ultrasound Med. Biol. **25**, 275–283 (1999).
- <sup>10</sup>J. K. Dave, S. V. Kulkarni, P. P. Pangaonkar, M. Stanczak, M. E. McDonald, I. S. Cohen, P. Mehrotra, M. P. Savage, P. Walinsky, N. J. Ruggiero II, D. L. Fischman, D. Ogilby, C. VanWhy, M. Lombardi, and F. Forsberg, "Non-invasive intra-cardiac pressure measurements using subharmonic-aided pressure estimation: Proof of concept in humans," Ultrasound Med. Biol. 43, 2718–2724 (2017).
- <sup>11</sup>J. R. Eisenbrey, J. K. Dave, V. G. Halldorsdottir, D. A. Merton, C. Miller, J. M. Gonzalez, P. Machado, S. Park, S. Dianis, C. L. Chalek, C. E. Kim, J. P. Baliff, K. E. Thomenius, D. B. Brown, V. Navarro, and F. Forsberg, "Chronic liver disease: Noninvasive subharmonic aided pressure estimation of hepatic venous pressure gradient," Radiology 268, 581–588 (2013).
- <sup>12</sup>K. Nam, J. R. Eisenbrey, M. Stanczak, A. Sridharan, A. C. Berger, T. Avery, J. P. Palazzo, and F. Forsberg, "Monitoring neoadjuvant chemotherapy for breast cancer by using three-dimensional subharmonic aided pressure estimation and imaging with US contrast agents: Preliminary experience," Radiology 285, 53–62 (2017).
- <sup>13</sup>I. Gupta, J. R. Eisenbrey, P. Machado, M. Stanczak, C. E. Wessner, C. M. Shaw, S. Gummadi, J. M. Fenkel, A. Tan, C. Miller, J. Parent, S. Schultz,

- M. C. Soulen, C. M. Sehgal, K. Wallace, and F. Forsberg, "Diagnosing portal hypertension with noninvasive subharmonic pressure estimates from a US contrast agent," Radiology **298**, 104–111 (2021).
- <sup>14</sup>C. Esposito, P. Machado, M. E. McDonald, M. P. Savage, D. Fischman, P. Mehrotra, I. S. Cohen, N. Ruggiero II, P. Walinsky, A. Vishnevsky, K. Dickie, M. Davis, F. Forsberg, and J. K. Dave, "Noninvasive evaluation of cardiac chamber pressures using subharmonic-aided pressure estimation with Definity microbubbles," JACC: Cardiovasc. Imaging 16, 224–235 (2023).
- <sup>15</sup>F. Forsberg, W. T. Shi, and B. B. Goldberg, "Subharmonic imaging of contrast agents," Ultrasonics 38, 93–98 (2000).
- <sup>16</sup>F. Forsberg, C. W. Piccoli, A. Sridharan, A. Wilkes, A. Sevrukov, H. Ojeda-Fournier, R. F. Mattrey, P. Machado, M. Stanczak, D. A. Merton, K. Wallace, and J. R. Eisenbrey, "3D harmonic and subharmonic imaging for characterizing breast lesions: A multi-center clinical trial," J. Ultrasound Med. 41, 1667–1675 (2022).
- <sup>17</sup>D. E. Goertz, M. E. Frijlink, D. Tempel, V. Bhagwandas, A. Gisolf, R. Krams, N. de Jong, and A. F. W. van der Steen, "Subharmonic contrast intravascular ultrasound for vasa vasorum imaging," Ultrasound Med. Biol. 33, 1859–1872 (2007).
- <sup>18</sup>J. R. Eisenbrey, A. Sridharan, P. Machado, H. Zhao, V. G. Halldorsdottir, J. K. Dave, J.-B. Liu, S. Park, S. Dianis, K. Wallace, K. E. Thomenius, and F. Forsberg, "Three-dimensional subharmonic ultrasound imaging in vitro and in vivo," Acad. Radiol. 19, 732–739 (2012).
- <sup>19</sup>J. R. Eisenbrey, A. Sridharan, J. B. Liu, and F. Forsberg, "Recent experiences and advances in contrast-enhanced subharmonic ultrasound," Biomed. Res. Int. 2015, 640397 (2015).
- <sup>20</sup>J. Chomas, P. Dayton, D. May, and K. Ferrara, "Nondestructive subharmonic imaging," IEEE Trans. Ultrason. Ferroelectr. Freq. Control 49, 883–892 (2002).
- <sup>21</sup>P. D. Krishna, P. M. Shankar, and V. L. Newhouse, "Subharmonic generation from ultrasonic contrast agents," Phys. Med. Biol. 44, 681–694 (1999).
- <sup>22</sup>K. Sarkar, W. T. Shi, D. Chatterjee, and F. Forsberg, "Characterization of ultrasound contrast microbubbles using in vitro experiments and viscous and viscoelastic interface models for encapsulation," J. Acoust. Soc. Am. 118, 539–550 (2005).
- <sup>23</sup>F. Forsberg, J. B. Liu, W. T. Shi, J. Furuse, M. Shimizu, and B. B. Goldberg, "*In vivo* pressure estimation using subharmonic contrast microbubble signals: Proof of concept," IEEE Trans. Ultrason. Ferroelectr. Freq. Control **52**, 581–583 (2005).
- <sup>24</sup>E. H. Chang, "An introduction to contrast-enhanced ultrasound for nephrologists," Nephron 138, 176–185 (2018).
- <sup>25</sup>G. Xu, H. Lu, H. Yang, D. Li, R. Liu, M. Su, B. Jin, C. Li, T. Lv, S. Du, J. Yang, W. Qiu, Y. Mao, and F. Li, "Subharmonic scattering of SonoVue microbubbles within 10–40-mmHg overpressures *in vitro*," IEEE Trans. Ultrason. Ferroelectr. Freq. Control 68, 3583–3591 (2021).
- <sup>26</sup>S. Liu, J. Wu, Y. Gu, X. Guo, J. Tu, D. Xu, and D. Zhang, "Ambient pressure evaluation through sub-harmonic response of chirp-sonicated microbubbles," Ultrasound Med. Biol. 43, 332–340 (2017).
- <sup>27</sup>A. Q. X. Nio, A. Faraci, K. Christensen-Jeffries, J. L. Raymond, M. J. Monaghan, D. Fuster, F. Forsberg, R. J. Eckersley, and P. Lamata, "Optimal control of SonoVue microbubbles to estimate hydrostatic pressure," IEEE Trans. Ultrason. Ferroelectr. Freq. Control 67, 557–567 (2020).
- <sup>28</sup>X. Qiao, Y. Wen, J. Yu, A. Bouakaz, Y. Zong, and M. Wam, "Noninvasive pressure estimation based on the subharmonic response of SonoVue: Application to intracranial blood pressure assessment," IEEE Trans. Ultrason. Ferroelectr. Freq. Control 69, 957–966 (2022).
- <sup>29</sup>I. Gupta, A. Q. X. Nio, A. Faraci, M. Torkzaban, K. chrostemsem-Jeffries, K. Nam, J. L. Raymond, K. Wallace, M. J. Monaghan, D. Fuster, and R. J. Eckersley, "The effects of hydrostatic pressure on the subharmonic response of SonoVue and Sonazoid," in 2019 IEEE International Ultrasonics Symposium (IUS), Glasgow, UK (6–9 October) (IEEE, New York), pp. 1349–1352, (2019).
- <sup>30</sup>C. Dockerill, A. Faraci, K. Christensen-Jeffries, J. Alastruey, R. Raiani, P. Lamata, and A. Q. X. Nio, "SonoVue microbubbles as ultrasound pressure sensors in a dynamic flow phantom," in 2021 IEEE International Ultrasonics Symposium (IUS), (2021), Xi'an, China (11–16 September) (IEEE, New York), pp. 1–4.
- <sup>31</sup>F. Li, D. Li, and F. Yan, "Improvement of detection sensitivity of microbubbles as sensors to detect ambient pressure," Sensors (Basel) 18, 4083 (2018).

- <sup>32</sup>K. S. Andersen and J. A. Jensen, "Impact of acoustic pressure on ambient pressure estimation using ultrasound contrast agent," Ultrasonics 50, 294–299 (2010).
- <sup>33</sup>P. J. Frinking, J. Brochot, and M. Arditi, "Subharmonic scattering of phospholipid-shell microbubbles at low acoustic pressure amplitudes," IEEE Trans. Ultrason. Ferroelectr. Freq. Control 57, 1762–1771 (2010).
- <sup>34</sup>R. H. Azami, F. Forsberg, J. R. Eisenbrey, and K. Sarkar, "Ambient pressure sensitivity of the subharmonic response of coated microbubbles: Effects of acoustic excitation parameters," Ultrasound Med. Biol. 49, 1550–1560 (2023).
- <sup>35</sup>N. de Jong, M. Emmer, C. T. Chin, A. Bouakaz, F. Mastik, D. Lohse, and M. Versluis, "'Compression-only' behavior of phospholipid-coated contrast bubbles," Ultrasound Med. Biol. 33, 653–656 (2007).
- <sup>36</sup>P. Marmottant, S. van der Meer, M. Emmer, M. Versluis, N. de Jong, S. Hilgenfeldt, and D. Lohse, "A model for large amplitude oscillations of coated bubbles accounting for buckling and rupture," J. Acoust. Soc. Am. 118, 3499–3505 (2005).
- <sup>37</sup>J. Sijl, B. Dollet, M. Overvelde, V. Garbin, T. Rozendal, N. de Jong, D. Lohse, and M. Versluis, "Subharmonic behavior of phospholipid-coated ultrasound contrast agent microbubbles," J. Acoust. Soc. Am. 128, 3239–3252 (2010).
- <sup>38</sup>J. Sijl, M. Overvelde, B. Dollet, V. Garbin, N. de Jong, D. Lohse, and M. Versluis, "'Compression-only' behavior: A second-order nonlinear response of ultrasound contrast agent microbubbles," J. Acoust. Soc. Am. 129, 1729–1739 (2011).
- <sup>39</sup>A. Kaushik, A. H. Khan, Pratibha, S. V. Dalvi, and H. Shekhar, "Effect of temperature on the acoustic response and stability of size-isolated protein-shelled ultrasound contrast agents and SonoVue," J. Acoust. Soc. Am. 153, 2324–2335 (2023).
- <sup>40</sup>C. Greis, "Technology overview: SonoVue (Bracco, Milan)," Eur. Radiol. 14(Suppl 8), P11–P15 (2004).
- <sup>41</sup>N. de Jong, M. Emmer, A. van Wamel, and M. Versluis, "Ultrasonic characterization of ultrasound contrast agents," Med. Biol. Eng. Comput. 47, 861–873 (2009).
- <sup>42</sup>C. Mannaris and M. A. Averkiou, "Investigation of microbubble response to long pulses used in ultrasound-enhanced drug delivery," Ultrasound Med. Biol. 38, 681–691 (2012).
- <sup>43</sup>B. L. Helfield, E. Cherin, F. S. Foster, and D. E. Goertz, "Investigating the subharmonic response of individual phospholipid encapsulated microbubbles at high frequencies: A comparative study of five agents," Ultrasound Med. Biol. 38, 846–863 (2012).
- <sup>44</sup>E. Kimmel, B. Krasovitski, A. Hoogi, D. Razansky, and D. Adam, "Subharmonic response of encapsulated microbubbles: Conditions for existence and amplification," Ultrasound Med. Biol. 33, 1767–1776 (2007).
- <sup>45</sup>E. Kanbar, D. Fouan, C. A. Sennoga, A. A. Doinikov, and A. Bouakaz, "Impact of filling gas on subharmonic emissions of phospholipid ultrasound contrast agents," Ultrasound Med. Biol. 43, 1004–1015 (2017).
- <sup>46</sup>K. Sarkar, A. Katiyar, and P. Jain, "Growth and dissolution of an encapsulated contrast microbubble: Effects of encapsulation permeability," Ultrasound Med. Biol. 35, 1385–1396 (2009).
- <sup>47</sup>A. Katiyar, K. Sarkar, and P. Jain, "Effects of encapsulation elasticity on the stability of an encapsulated microbubble," J. Colloid Interface Sci. 336, 519–525 (2009).
- <sup>48</sup>A. Prosperetti, "A general derivation of the subharmonic threshold for non-linear bubble oscillations," J. Acoust. Soc. Am. 133, 3719–3726 (2013).
- <sup>49</sup>T. Sun, N. Jia, D. Zhang, and D. Xu, "Ambient pressure dependence of the ultra-harmonic response from contrast microbubbles," J. Acoust. Soc. Am. 131, 4358–4364 (2012).
- <sup>50</sup>I. Gupta, J. R. Eisenbrey, P. Machado, M. Stanczak, K. Wallace, and F. Forsberg, "On factors affecting subharmonic-aided pressure estimation (SHAPE)," Ultrason. Imaging 41, 35–48 (2019).
- <sup>51</sup>J. K. Dave, V. G. Halldorsdottir, J. R. Eisenbrey, D. A. Merton, J. B. Liu, P. Machado, H. Zhao, S. Park, S. Dianis, C. L. Chalek, K. E. Thomenius, D. B. Brown, and F. Forsberg, "On the implementation of an automated acoustic output optimization algorithm for subharmonic aided pressure estimation," Ultrasonics 53, 880–888 (2013).
- <sup>52</sup>P. Machado, I. Gupta, S. Gummadi, M. Stanczak, C. E. Wessner, J. M. Fenkel, C. M. Shaw, S. Shamini-Noori, S. Schultz, M. C. Soulen, C. M. Sehgal, K. Wallace, J. R. Eisenbrey, and F. Forsberg, "Hepatic vein

## JASA

#### https://doi.org/10.1121/10.0025690

contrast-enhanced ultrasound subharmonic imaging signal as a screening test for portal hypertension," Dig. Dis. Sci. 66, 4354–4360 (2021).

<sup>53</sup>V. G. Halldorsdottir, J. K. Dave, L. M. Leodore, J. R. Eisenbrey, S. Park, A. L. Hall, K. Thomenius, and F. Forsberg, "Subharmonic contrast microbubble signals for noninvasive pressure estimation under static and dynamic flow conditions," Ultrason. Imaging 33, 153–164 (2011).

<sup>54</sup>V. G. Halldorsdottir, J. K. Dave, J. R. Eisenbrey, P. Machado, H. Zhao, J. B. Liu, D. A. Merton, and F. Forsberg, "Subharmonic aided

pressure estimation for monitoring interstitial fluid pressure in tumours—*In vitro* and *in vivo* proof of concept," Ultrasonics **54**, 1938–1944 (2014).

<sup>55</sup>J. K. Dave, V. G. Halldorsdottir, J. R. Eisenbrey, J. B. Liu, M. E. McDonald, K. Dickie, C. Leung, and F. Forsberg, "Noninvasive estimation of dynamic pressures in vitro and in vivo using the subharmonic response from microbubbles," IEEE Trans. Ultrason. Ferroelectr. Freq. Control 58, 2056–2066 (2011).